Experimental and numerical analysis of wrinkling during forming of multilayered textile composites

E. Guzman-Maldonado, P. Wang, N. Hamila, P. Boisse

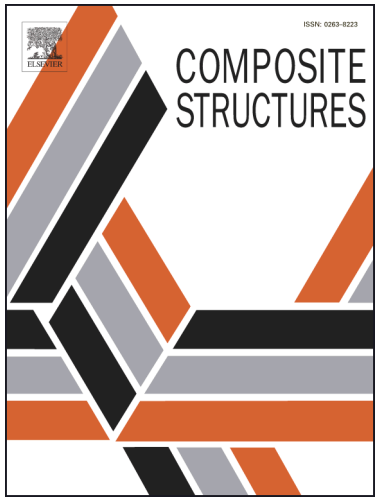

Experimental and numerical analysis of wrinkling during forming of multi-layered textile composites

E. Guzmán-Maldonado, P. Wang, N. Hamila, P. Boisse

PII: S0263-8223(18)31432-6
DOI: https://doi.org/10.1016/j.compstruct.2018.10.018
Reference: COST 10268

To appear in: *Composite Structures*

Received Date: 17 April 2018
Revised Date: 7 August 2018
Accepted Date: 4 October 2018

Please cite this article as: Guzmán-Maldonado, E., Wang, P., Hamila, N., Boisse, P., Experimental and numerical analysis of wrinkling during forming of multi-layered textile composites, *Composite Structures* (2018), doi: https://doi.org/10.1016/j.compstruct.2018.10.018

Experimental and numerical analysis of wrinkling during forming of multi-layered textile composites

E. Guzmán-Maldonado[1], P. Wang[2], N. Hamila[1], P. Boisse[1*]

[1]*Université de Lyon, LaMCoS, INSA-Lyon, F-69621, France*

[2] *Université de Lille, GEMTEX, ENSAIT, F-59056 Roubaix, France*

Abstract

Wrinkling is one of the main flaws that can appear during forming processes of textile composite reinforcements. When the forming is carried out on a multi-layered fabric the wrinkle development is strongly increased if the plies have different orientations. This phenomenon has been observed in previous experimental studies and is confirmed by a set of forming tests on multi-layered reinforcements. Beyond these experiments, a multilayered fabric forming process numerical simulation based on stress-resultant textile shell elements is presented. It is shown that this simulation is able to accurately describe multi-layered fabric forming processes and in particular the development of wrinkles. In the case of multi-layered reinforcements where the neighboring plies are oriented differently, the numerical simulations shows the development of zones where the fibers in one direction are subjected to compression which gives rise to wrinkles. The analysis of the forming for different friction coefficients confirms the major role of the friction between the plies in wrinkling. The influence of the pressure imposed by the blank holder has also been studied.

Key words: Fabrics/textiles, Wrinkling, Multi-layer, Composite reinforcements, Friction, Computational modelling;

*Corresponding author.
E-mail address: philippe.boisse@insa-lyon.fr (P. Boisse).

1. Introduction.

Wrinkles are one of the most common manufacturing-induced defects when forming a textile composite reinforcement or prepreg. The simulation codes that are used to determine the feasibility of the manufacturing processes must be able to determine the onset and development of wrinkles. The objective of these simulations is to determine the process parameters that prevent wrinkling of the composite at the end of the forming. Scientific studies on wrinkling of fiber reinforcements are numerous and many are recent. Wrinkling is a major issue for any kind of sheet forming regardless of the nature of the materials [1-5]. Fibrous reinforcements and prepregs are particularly prone to wrinkling because of the fibrous composition and the possible slippage between the fibers that precipitate these defects [6-9]. Their analysis and simulation is therefore particularly important.

The wrinkles of woven textile reinforcements have been related to in-plane shear in studies based on the 'shear locking angle' which, for woven reinforcements, is an angle between warp and weft yarns beyond which wrinkling appears (according to this approach) [10-18]. Recent studies have aimed to refine these analyses, in particular by mesoscopic simulations of in-plane shear [19-22] and to question the notion of a shear-locking angle [23, 24]. Numerical simulations of wrinkling have also been based on models of beams and membranes [25-29].

While this paper considers wrinkling of woven reinforcements (multilayer), a significant number of studies have been devoted to the wrinkling of unidirectional (UD) reinforcements and prepregs during manufacturing [30-42]. The mechanical behavior of such UD reinforcements made of parallel fibers is specific. The very large difference in rigidity between the orientation of the fibers and the transverse direction may lead to wrinkles related to the bridging of the rigid ply and the friction during consolidation under autoclave pressure [31]. Wrinkling can also occur during consolidation over an external radius [41,42].

This article considers the wrinkles of woven fibrous reinforcements. More particularly, it analyzes the interactions between the different layers during forming and their consequences

on wrinkling. The potential for the formation of wrinkles is increased when the preform is multi-layered, especially when the layers have different orientations. This particular behavior has been previously reported by some authors in the case of composite reinforcements and prepregs for different geometries and stacking configurations [43-49]

Vanclooster et al. carried out an experimental study on wrinkle formation during thermoplastic prepreg thermoforming for different ply orientations [45]. Wrinkling was analyzed using a kinematic draping solution of a single layer in different orientations. Some trends were highlighted. However, kinematical simulations do not take into account the mechanical properties of the reinforcement and friction properties and thus do not necessarily correlate with reality. Ten Thije et al. analyzed this problem using a multi-layered membrane finite element and proposed a wrinkling indicator based on the local stress state [44]. Inter-ply friction was taken into account, but they used a membrane element which could not describe the geometry of the wrinkles. The authors acknowledged that shell elements should be used.

The present paper first describes an experimental study of wrinkling during the forming of multi-layered woven reinforcements with different ply orientations. This study confirmed that stacking with different orientations of the plies led to significant wrinkling.

Beyond these experiments, the objective of this article is to present relevant simulations of the forming of multi-ply reinforcements and use them to analyze the reasons for wrinkling. These simulations are based on the modelling of the fabric layers in contact by stress-resultant shell finite elements. The results of the numerical analyses were consistent with the forming experiments. The simulation showed that when forming with different ply stack orientations, the interply slip (or the tendency to slip) and the friction gave rise to compression loads in the fiber direction and to wrinkles. The significance of the role of interply and tool/ply friction is explored. Finally, the effect of the pressure applied by a blank holder was analyzed in the case of forming of multi-layered reinforcements.

2. Wrinkling during forming of textile composite reinforcements.

The analysis of wrinkling of woven composite reinforcements during a forming process is based on an explicit scheme and a simplified form of the internal virtual work. Dynamic explicit approaches [50, 51] are well suited for shaping simulations especially when such forming lead to wrinkling.

The virtual work theorem relates the internal, exterior, contact and acceleration virtual works. In a virtual displacement field $\boldsymbol{\eta}$ where $\boldsymbol{\eta}$=0 at the boundary with a prescribed displacement:

$$W_{ext}(\boldsymbol{\eta}) - W_{int}(\boldsymbol{\eta}) - W_{c}(\boldsymbol{\eta}) = W_{acc}(\boldsymbol{\eta}) \quad (1)$$

In the case of a woven fabric, the internal virtual work can be considered to be the sum of the virtual work of tension $W_{int}^{tens}(\boldsymbol{\eta})$, the virtual work of in-plane shear $W_{int}^{shear}(\boldsymbol{\eta})$ and the virtual work of bending $W_{int}^{bend}(\boldsymbol{\eta})$:

$$W_{int}(\boldsymbol{\eta}) = W_{int}^{tens}(\boldsymbol{\eta}) + W_{int}^{shear}(\boldsymbol{\eta}) + W_{int}^{bend}(\boldsymbol{\eta}) \quad (2)$$

Shell finite elements made of textile woven cells can be built based on Equation (2) from tensile, in-plane shear and bending behaviors [52, 53]. Eq. (2) renders it possible to study the influence of the different stiffnesses (tension, in-plane shear, bending) during the onset and development of wrinkles [23, 54-59]. For instance, Fig. 1 presents a woven textile reinforcement draped on a cylindrical punch. In Fig. 1a, only the tensile stiffness is non-zero. The simulation does not show any wrinkling. The in-plane shear angles are very large in the corners of the fabric blank. The simulation leads to wrinkles when an in-plane shear stiffness is added (Fig. 11(b)). These wrinkles are numerous and very small. Taking into account all the rigidities (i.e., adding the bending stiffness to the tensile and in-plane shear stiffnesses) leads to a deformed shape with larger wrinkles in good agreement with reality (Fig. 1(c)). Globally, the tensile, in-plane shear and bending stiffnesses play a role in the onset and development of wrinkles during the forming of a textile composite reinforcement. The tensile stiffness is large and leads to a deformed shape with a quasi-inextensibility in the fiber direction. The bending stiffness determines the size of the wrinkles. The in-plane shear angle required to reach a double curve shape is often the cause

of wrinkling. Nevertheless, Eq. (2) concerns the three rigidities (tension, in-plane shear and bending). This equation can either lead to wrinkling (i.e., an out-of-plane solution) or not, depending on all the terms. For example, very large shear angles can be reached without wrinkling when a high tension is created by a blank holder [23].

The present section has considered a single-layer woven reinforcement. The subsequent sections analyze how the interactions of the layers of a laminate modify the wrinkling onset and development during a forming process.

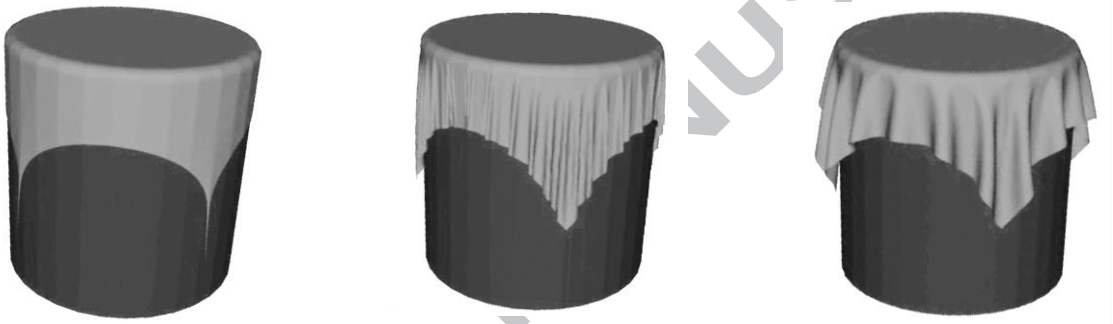

(a) (b) (c)

Fig. 1 Simulation of draping on a cylindrical punch. (a) Tensile stiffness only, (b) Tensile and in-plane shear stiffnesses (c) Tensile, in-plane shear and bending stiffnesses.

3. Experimental analyses of wrinkling in multi-layered textile composite reinforcements.

Experimental forming tests were performed on multi-layered dry textile reinforcements in order to analyze the influence of stacking on wrinkle formation.

3.1. Material and lay-up configurations.

A balanced plain-weave fabric made of continuous fiberglass was used for each layer. The principal fabric properties are listed in Table 1. The dimensions of a single ply were 400 mm x 400 mm x 0.135 mm.

Table 1. Principal fabric parameters

Properties		Units
Weave style	Plain weave	
Area density	160	[g/m²]
Type of yarn	Glass-EC968	
Warp	11.8	Yarns/cm
Weft	10.7	Picks/cm
Weight distribution	Warp: 52 Weft: 48	%
Thickness	0.135	[mm]

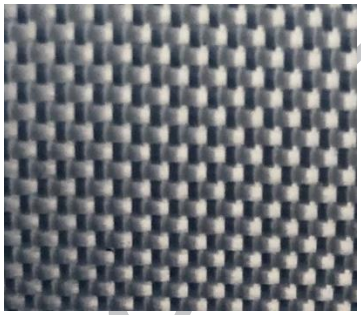

.

Different material configurations were investigated. As a first step, the forming of a single ply was considered for orientations of [0°/90°] and [-45°/45°] relative to the blank. Secondly, a stack of four layers was considered for three different configurations: $[0°/90°]_4$, $[-45°/45°]_4$ and a quasi-isotropic lay-up $[0°/90°,-45°/45°]_2$. These configurations are summarized in Table 2.

Table 2. Lay-up configurations.

Configuration	Number of plies	Lay-up	
C_1	1	[0°/90°]	
C_2	1	[-45°/45°]	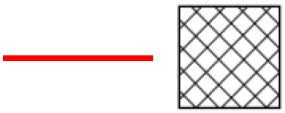
C_3	4	$[0°/90°]_4$	
C_4	4	$[-45°/45°]_4$	
C_5	4	$[0°/90°, -45°/45°]_2$	

3.2 Forming process

Forming experiments were carried out using a hemispherical punch as shown in Fig. 2. The blank holder applied a pressure of 0.05 MPa to the outer part of the blank during the forming

stage. The punch performed a vertical displacement at a constant rate of 30 mm/min with a maximum displacement of 75 mm.

3.3 Experimental analysis

Fig. 3 shows the final deformed parts obtained for configurations C_1 and C_2. The preforms in Fig. 3a for a single layer at [0°/90°] and in Fig. 3b for a single layer at [-45°/45°] are free of wrinkles.

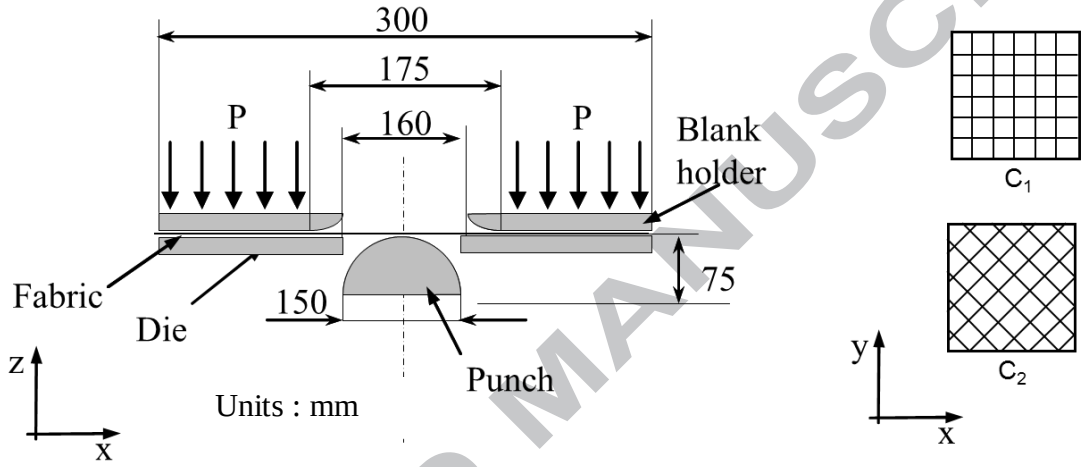

Fig. 2. Geometry and dimensions of the experimental forming test.

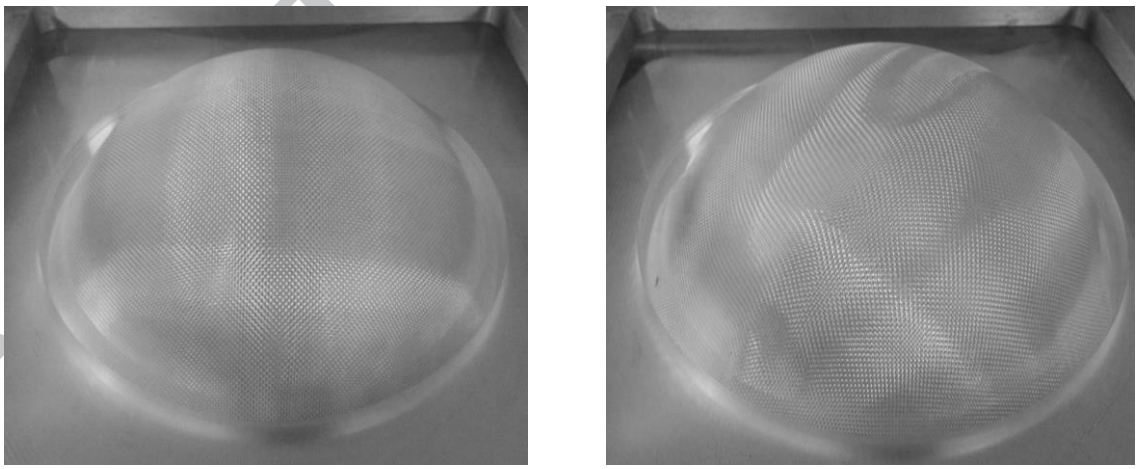

(a) (b)

Fig. 3. Hemispherical forming of a single layer at (a) [0°/90°] and (b) [-45°/45°]

In a subsequent step, the same forming experiments were repeated using four layers of reinforcements with four plies at [0°/90°] (Configuration C_3) and with four plies at [-45°/45°]

(Configuration C_4). The objective was to analyze wrinkles in multilayer textile reinforcements when all the layers had the same orientation.

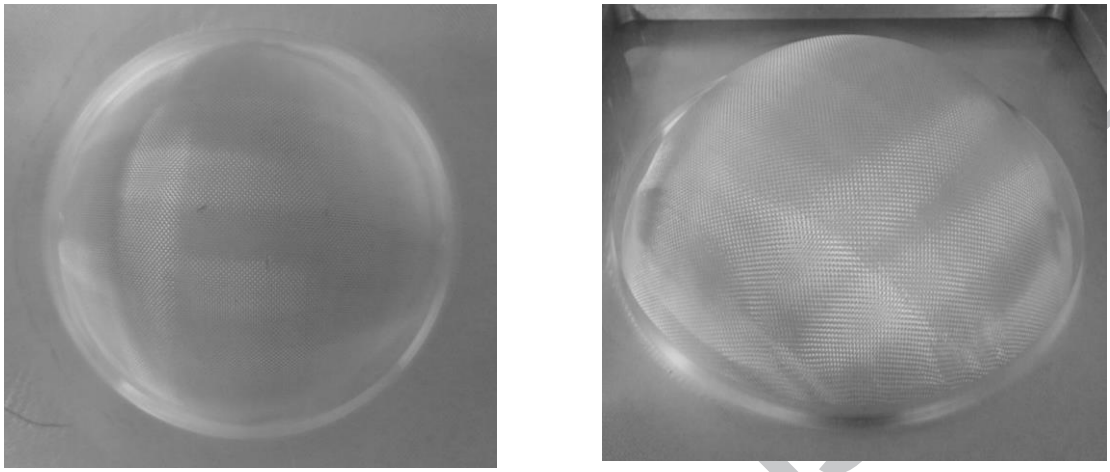

(a) (b)

Fig. 4. Hemispherical forming of 4 plies at (a) $[0°/90°]_4$ and with 4 plies at (b) $[-45°/45°]_4$

Fig. 4a and Fig. 4b show that the preforms with plies oriented in the same direction were free of wrinkles (small wrinkles could appear at the base of the hemisphere). The last experiment involved the forming of the quasi-isotropic lay-up (Configuration C_5, $[0°/90°, -45°/45°]_2$). In this case, numerous wrinkles of high amplitude developed in a large part of the hemispherical preform (Fig. 5). These wrinkles affected all layers of the preform.

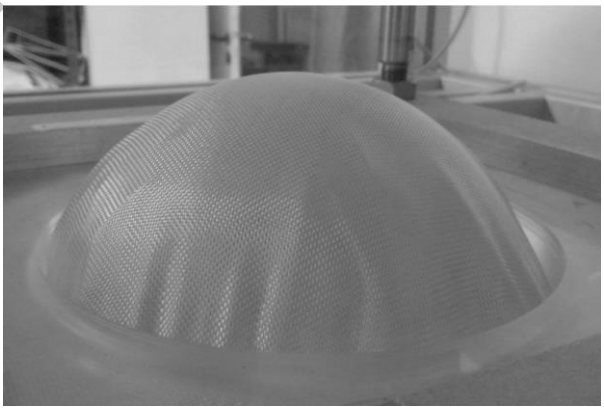

Fig. 5. Forming of the quasi-isotropic lay-up (Configuration C5, $[0°/90°, -45°/45°]_2$)

The experiments presented above show that the quasi-isotropic lay-up was a very significant factor for the onset and development of wrinkles during forming. Slippage between neighboring

plies that were oriented differently was necessary for the forming and was critical for the wrinkling. This observation was in agreement with previous investigations [44, 45].

The next sections demonstrate to what extent simulations of the forming and wrinkling of multi-layered fabric composites can predict the onset and development of wrinkles, and also analyze the reasons for wrinkling and determine the influence of certain parameters.

3.4 Wrinkling mechanism in multi-layered reinforcements

The specific development of wrinkles during the forming of multilayer reinforcements is due to friction and the possible local compression that results. Because, the deformation is not the same for two neighboring layers with different orientations, a relative sliding occurs. If this slip movement is constrained because of friction, tangential forces are generated at the contact interfaces thereby inducing a possible local wrinkling of the plies in contact. In some thermoplastic prepreg thermoforming, the interply slip can be almost nil for quasi isotropic laminates [44]. In the case of the quasi-isotropic lay-up forming shown Fig. 5, the interply slip is not equal to zero but it is reduced compared to that of a frictionless forming. (This point will be addressed in the next section).

4. Numerical Simulation

The present work has analyzed the wrinkling mechanism of multilayer reinforcements using a stress-resultant textile shell finite element. The shells represent woven reinforcements with warp and weft directions [52]. First, a set of simulations intended to analyze the forming tests presented in section 3 is described. These simulations should render an inside understanding of the wrinkle development by analyses of internal forces in the plies. The influence of friction and the blank holder pressure are then described.

3.5 Stress-resultant textile shell element analyses

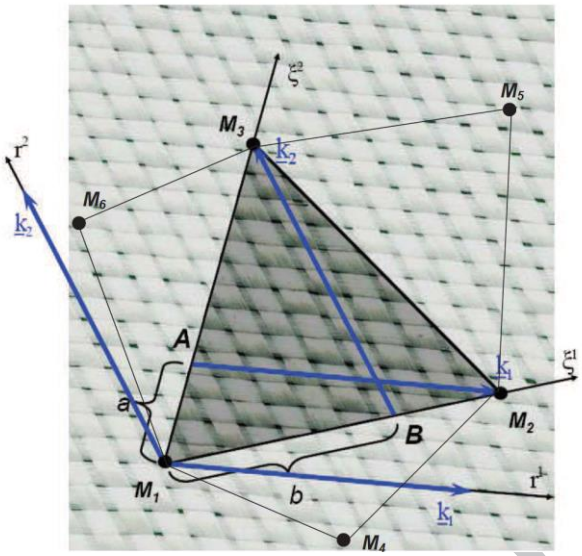

Fig. 6. Shell element made of woven cells.

The internal work results from those of the woven cells that constitute the element (Fig. 6) [52]. The membrane and bending stiffnesses are decoupled. In a virtual displacement field $\boldsymbol{\eta}$, the tensile, in-plane shear and bending internal virtual works (Eq.(2)) are calculated as follows:

$$W_{int}^{tens}(\boldsymbol{\eta}) = \sum_{p=1}^{ncell} {}^{p}\varepsilon_{11}(\boldsymbol{\eta})\ {}^{p}T^{11}\ {}^{p}L_1 + {}^{p}\varepsilon_{22}(\boldsymbol{\eta})\ {}^{p}T^{22}\ {}^{p}L_2 \tag{3}$$

$$W_{int}^{shear}(\boldsymbol{\eta}) = \sum_{p=1}^{ncell} {}^{p}\gamma(\boldsymbol{\eta})\ {}^{p}M^{s} \tag{4}$$

$$W_{int}^{bend}(\boldsymbol{\eta}) = \sum_{p=1}^{ncell} {}^{p}\chi_{11}(\boldsymbol{\eta})\ {}^{p}M^{11}\ {}^{p}L_1 + {}^{p}\chi_{22}(\boldsymbol{\eta})\ {}^{p}M^{22}\ {}^{p}L_2 \tag{5}$$

where $ncell$ is the total number of woven cells, $\varepsilon_{11}(\boldsymbol{\eta})$ and $\varepsilon_{22}(\boldsymbol{\eta})$ are the virtual axial strains, $\gamma(\boldsymbol{\eta})$ is the virtual shear angle, $\chi_{11}(\boldsymbol{\eta})$ and $\chi_{22}(\boldsymbol{\eta})$ are the virtual curvatures in the warp and weft directions. A biaxial tensile test gives the tensions in the warp and weft fiber directions T^{11} and T^{22} as a function of the axial strain ε_{11} and ε_{22}. A picture frame test or the bias extension test gives the shear moment M_s as a function of the angle variation γ between the warp and weft yarns [24]. Finally, bending tests give the bending moments M^{11} and M^{22} as a function of respectively χ_{11} and χ_{22}, i.e., the curvatures of the warp and weft yarns.

The three node triangle shown Fig. 6 is composed of woven cells. The kinematics of the element is simply defined by the displacement of the three nodes. The degrees of freedom of the element are only the three components of the displacement vector in each of the three nodes. The displacement **u** of a point P within the element is interpolated from the nodal displacement:

$$\mathbf{u}(P) = \sum_{i=1}^{3} N_i \mathbf{u}(M_i) \qquad \text{with} \quad N_1 = 1 - \xi_1 - \xi_2 \qquad N_2 = \xi_1 \qquad N_3 = \xi_3 \qquad (6)$$

ξ_1, ξ_2 are the natural coordinates. At nodes M_1, M_2, M_3, (Fig. 6) they take the following values: $M_1(0,0)$, $M_2(1,0)$, $M_3(0,1)$. N_i are the standard linear interpolation functions.

The expressions of the virtual works Eq (3) to (5) associated with the interpolation Eq.(6) give the elementary internal nodal forces of tension, plane shear and bending [52].

For the purposes of numerical efficiency, bending stiffness is taken into account without introducing any degree of freedom of rotation. The present shell finite element is of the type 'rotation free' [60, 61]. The curvatures that appear in the virtual bending work (Eq. 5) are estimated from the position of the element (given by M_1, M_2, M_3, Fig. 6) and that of the neighbouring elements (given by M_4, M_5, M_6, Fig. 6). The calculation of the curvature in the warp (material coordinate r_1) and weft (material coordinate r^2) directions in function of the nodal displacement of the six nodes M_1 to M_6 is given in [52].

3.6 Numerical analysis of the forming

Each fabric layer is discretized using 10,000 shell finite elements. The material parameters of one single ply of the textile reinforcement are given in Table 3. Ply-to-ply and tool-to-ply Coulomb friction coefficients have been measured and were assumed to be constant (Table 3) [48, 62]. The constitutive behaviours are given by the relationships $T^{11}(\varepsilon_{11})$, $T^{22}(\varepsilon_{22})$, $M_s(\gamma)$, $M^{11}(\chi_{11})$, $M^{22}(\chi_{22})$, (Eq. (3) to (5)). They may be linear or non-linear depending on the results of the identification tests. In table 3, and for the analyses presented below, the in-plane shear behaviour is non-linear. Tension and bending behaviour are linear for simplicity.

Given the symmetry of the stacking configuration and the part, only one quarter of the structure is modelled using the corresponding symmetry conditions. The speed of the rigid punch surface is set to 5 mm/s. The maximal time step is 1.5 10^{-4} s and number of times steps equal to 10^5 . The CPU time required for these simulations depends on both the number of layers and the number of elements in each layer. Computation times range from 15 minutes to 20 hours (CPU @ 2.9 Ghz).

Table 3. Principal mechanical properties of the material and the corresponding experimental methods.

Mechanical Properties		Units	Measured by
Tensile $T^{11}=C_1\varepsilon_{11}$; $T^{22}=C_2\varepsilon_{22}$	$C_1= C_2=1000$	[N/Yarns]	Biaxial tensile test
In-plane shear $M^s=K_1\gamma+K_2\gamma^3+K_3\gamma^5$	$K_1= 0.371$ $K_2=-0.841$ $K_3= 1.013$	[N mm]	Bias-extension test
Bending $M^{11}=B_1\chi_{11}$; $M^{22}=B_2\chi_{22}$	$B_1= B_2=0.5$	[N mm]	Cantilever test
Friction Ply-to-ply (Coulomb coefficient) Tool-to-ply (Coulomb coefficient)	 0.21 0.23		Friction test

3.7 Influence of stacking sequence

Fig. 7 shows the computed deformed shape in the case of hemispherical forming of a single ply for configurations C_1 [0°/90°] and C_2 [-45°/45°]. The maximal computed shear angle for configuration C_1 was 42.2° as compared to 43.3° found experimentally and 42.8° for configuration C_2 as compared to 43.8°. Thus, the models and experiments compared well. The development of wrinkles was not observed for either of the simulations.

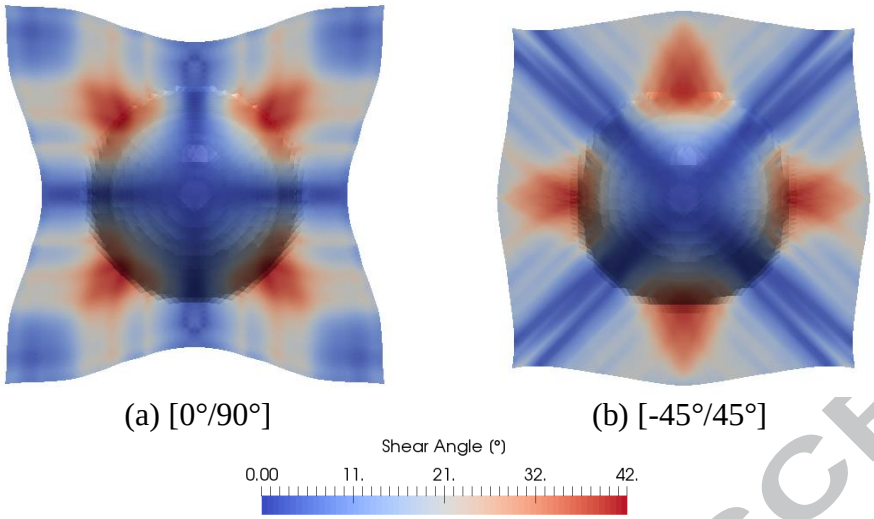

(a) [0°/90°] (b) [-45°/45°]

Fig. 7. Simulation of the hemispherical forming of a single ply.

The forming simulations were carried out for multilayer configurations C_3 (Four plies at [0°/90°] and C_4 (Four plies at [-45°/45°]). Fig. 8b and Fig. 8d show the deformed outer layer for these configurations. The simulations did not show any wrinkling development, which was in agreement with the experiments (Fig. 3 and 4).

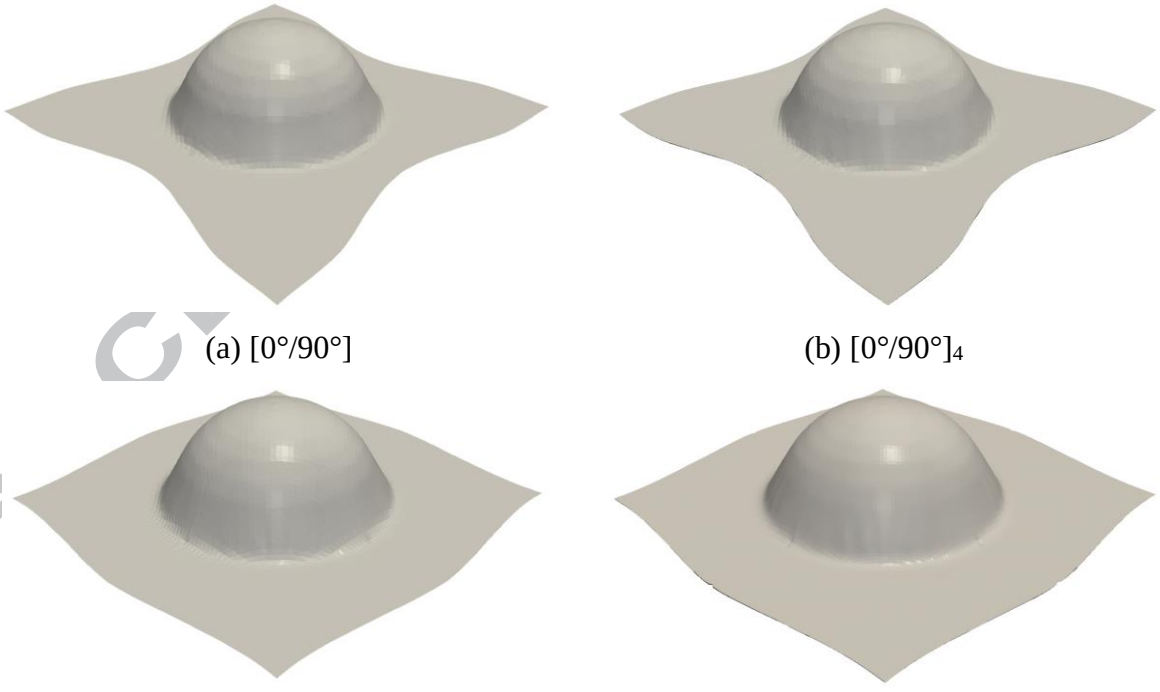

(a) [0°/90°] (b) $[0°/90°]_4$

(c) [-45°/45°] (d) $[-45°/45°]_4$

Fig. 8. Simulations of single and multi-layered forming with identical orientations.

Fig. 9 shows a comparison between the predicted and experimental final shape in the case of the quasi-isotropic lay-up (Configuration C_5). For this lay-up configuration, the simulation

gives numerous and large wrinkles. The localization of the onset and the geometry of the wrinkles in the part were in good agreement with the forming test (Fig. 9a and b).

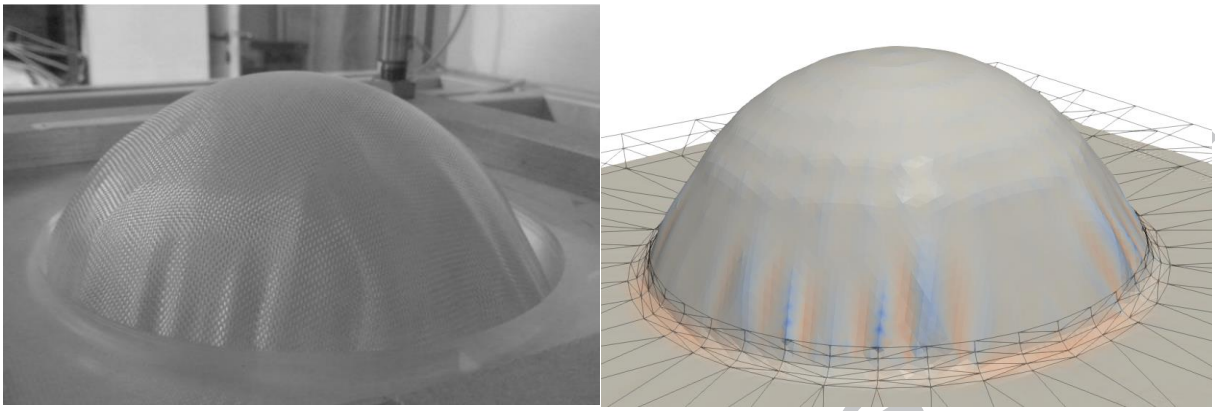

(a) (b)

Fig. 9. Experimental and numerical comparison of the distribution of wrinkles for quasi-isotropic stacking.

As can be seen in Fig. 10, the wrinkles extended through each layer of the part. Ply no. 1 and Ply no. 4 corresponded respectively to the inner and outer layers of the part. The intermediate layers (Fig. 10d and Fig. 10d) were slightly more affected by wrinkling.

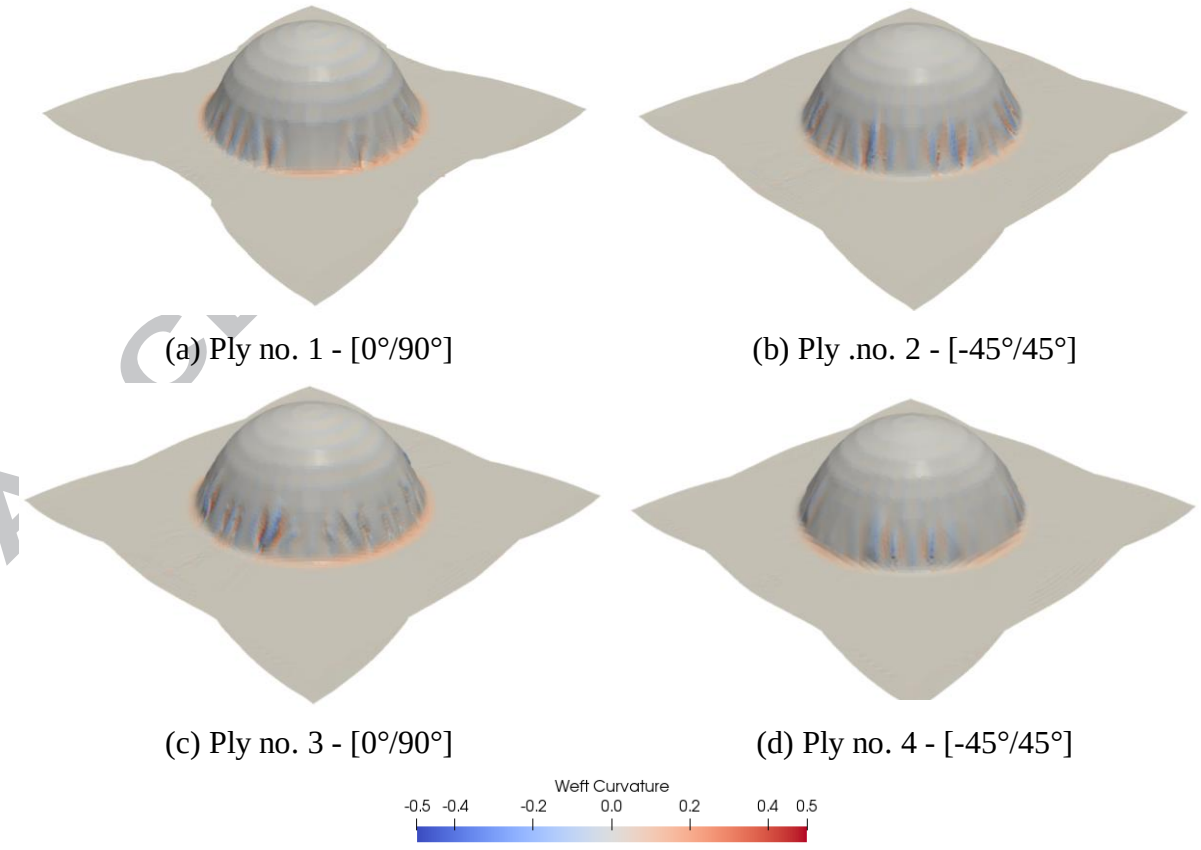

(a) Ply no. 1 - [0°/90°] (b) Ply .no. 2 - [-45°/45°]

(c) Ply no. 3 - [0°/90°] (d) Ply no. 4 - [-45°/45°]

Fig. 10. The development of wrinkles for each layer during forming in a quasi-isotropic lay-up.

3.8 Wrinkling mechanism for stacking with different ply orientations

To analyze the wrinkling mechanism of the quasi-isotropic lay-up, the distribution of the tensions along the yarn directions was evaluated for the second layer halfway through the forming process. The deformation during forming of the second layer, oriented at [-45°/45°], and of the neighboring layers, oriented at [0°/90°], was different. Interply slip and friction induced tangential contact forces, and Fig. 11 shows the normalized tensions along the warp and weft directions in the second layer. (The normalized tension is the tension in a yarn divided by the maximum tension value in the ply). Regarding the tensions generated in the weft yarns (Fig. 11b), one can notice that a compression zone was induced by the frictional forces, thus triggering the development of wrinkles. When a woven fabric is subjected to compression in the yarn direction it tends to buckle. The bending strain energy induced by this buckling is much smaller than the energy needed to compress the yarns [23]. In addition, it can be seen (Fig. 11b) that these wrinkles were oriented and propagated according to the direction of the warp tensions. In plane compressive load was the basic mechanism for wrinkle development when the layers had different orientations. Nevertheless, the wrinkles in the different layers were linked by the geometry and were close to each other for shape in the different plies.

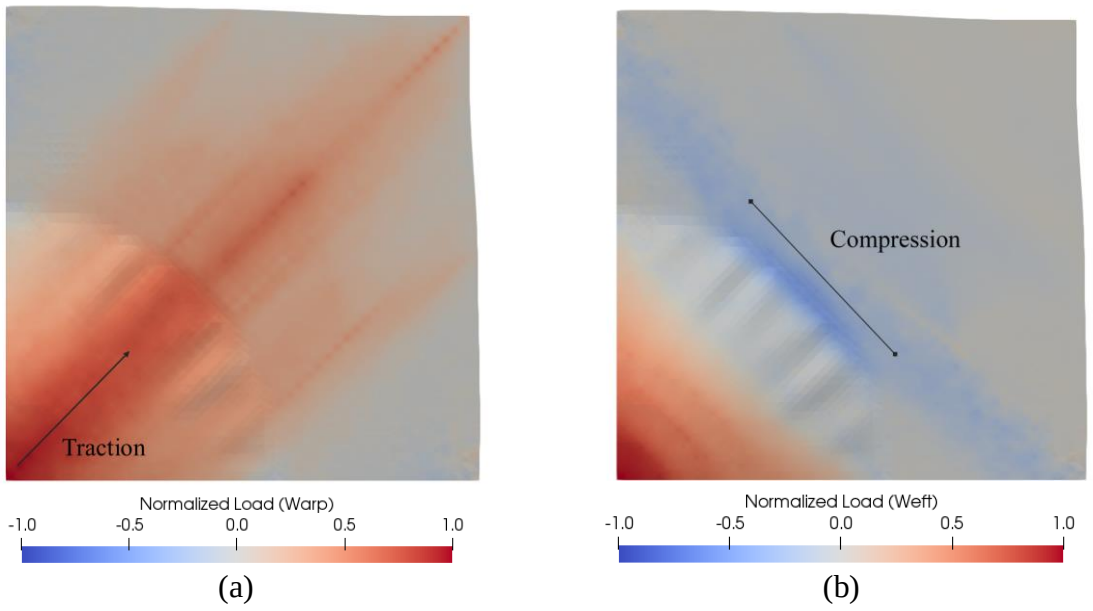

Fig. 11. Wrinkling mechanism for Ply no. 2. Normalized (a) warp and (b) weft tensions.

4.5 Influence of inter-ply friction

The importance of friction can be underlined by conducting a frictionless simulation and simulations with different friction coefficients. Fig. 12 shows the normalized compression force distribution obtained in the second ply for a friction coefficient equal to zero. As can be noted, compression in the fiber zones was minimal, resulting in the formation of almost no wrinkles (Fig. 12a). On the other hand, when the friction coefficient was increased (Fig. 12b and c), the compression forces became more significant. Consequently, the number of wrinkles increased as did their amplitude with increasing friction. Fig. 13 shows the final shape of the part as a function of the friction coefficient.

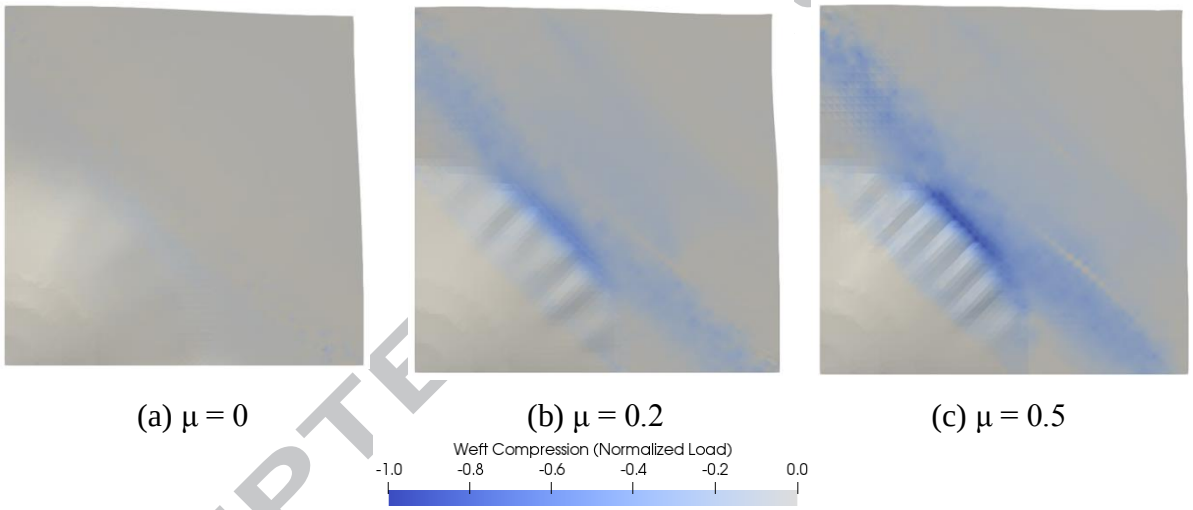

(a) $\mu = 0$ (b) $\mu = 0.2$ (c) $\mu = 0.5$

Fig. 12. Compression forces in ply no. 2 as a function of the friction coefficient.

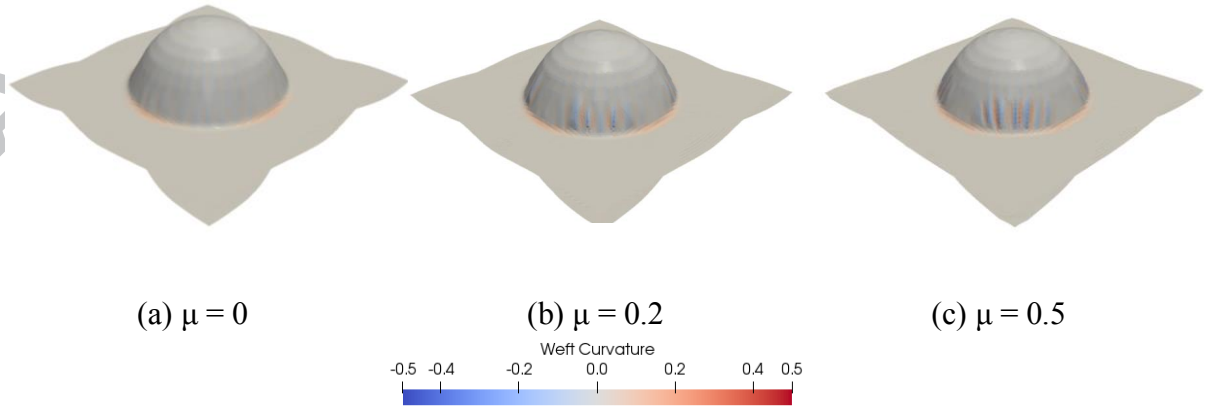

(a) $\mu = 0$ (b) $\mu = 0.2$ (c) $\mu = 0.5$

Fig. 13. Influence of the friction coefficient on the wrinkle development during the final stage.

Finally, the influence of friction on the interply slip was analyzed by looking at the position of the edge of each ply after forming. Fig. 14 shows that the interply slip is modified by friction. In the absence of friction (Fig. 14a), the deformed shape is that of a single ply at (0°/90°) for plies 1 and 3 and that of a ply at (-45°/45°) for folds 2 and 4. This deformation behaviour is no longer true when friction increases. The inter-ply slip is modified. In particular the central ply 3 oriented at (0°/90°), presents a limited slip compared to its neighbors 2 and 4 oriented at (-45°/45°) (Fig. 14b and c). Some studies have shown that this restriction of the interply slip may become total (no slippage) in the case of thermoforming of quasi-isotropic prepreg laminates [44]. For these materials, friction depends on the melting matrix which can lead to high values [63, 64]

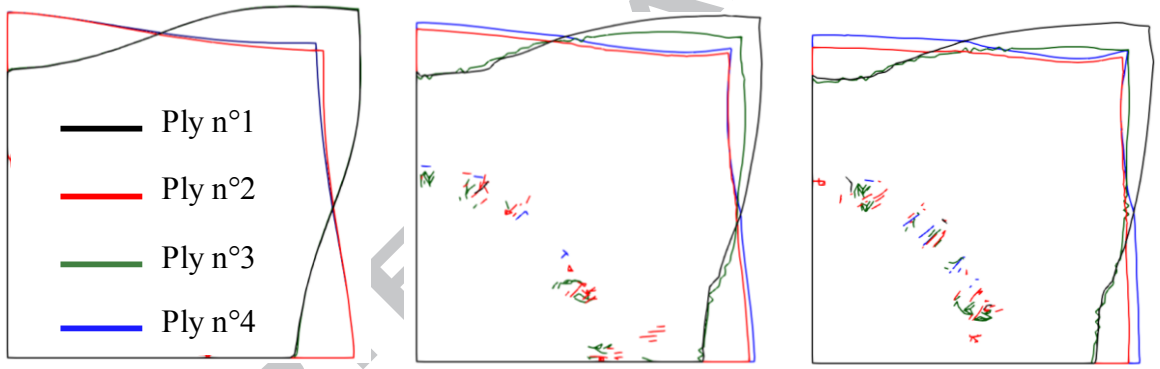

(a) μ = 0 (b) μ = 0.2 (c) μ = 0.5

Fig. 14. Influence of the friction coefficient on the interply slip

4.6 Influence of blank holder pressure

A blank-holder is a common device in sheet metal forming. It is also sometimes used for textile composites and prepreg forming. Its primary function is to reduce the occurrence of wrinkles during forming by inducing tension forces in the yarns through friction between the fabric and the holder [65-68]. These tension forces are proportional to the normal holder pressure and depend on the local relative orientation of the fabric. However, recent studies have shown that the use of this technique is not always effective in the case of multilayer fabrics exhibiting significant relative inter-ply slip during forming [48, 49].

To evaluate the influence of this parameter, a simulation was performed using the configuration C_5 and with the holder pressure cut in half. The friction coefficient was fixed to μ=0.21. Fig. 15 presents the compression forces in the yarn direction in ply no. 2 for two different pressure values. One could expect that the number of wrinkles and their amplitude would increase when the blank holder pressure decreased. However, as can be observed, the reduction of the holder pressure resulted in a lower number of wrinkles for this layer (Fig. 15b). The contact forces between layers decrease therefore the effects of the local interactions (compression forces induced by friction which are the cause of wrinkling) were reduced.

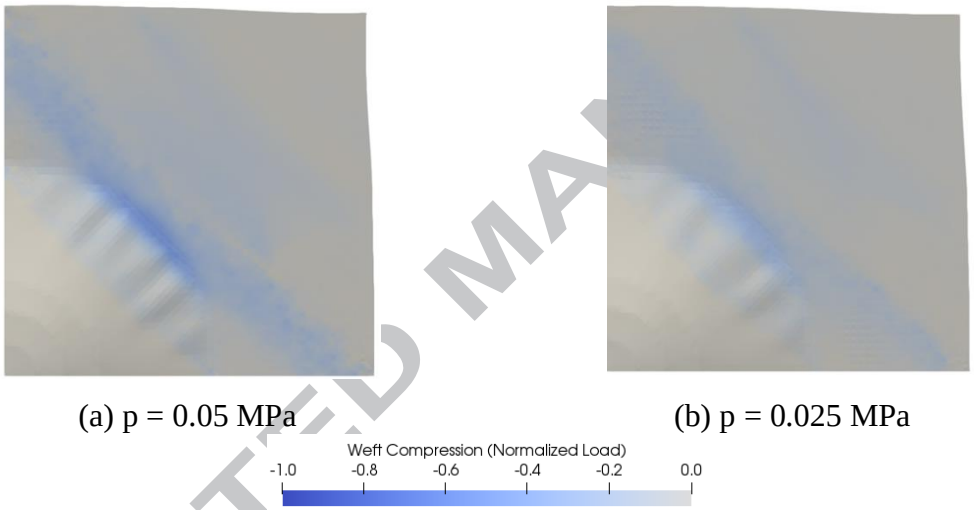

(a) p = 0.05 MPa (b) p = 0.025 MPa

Fig.15. Compression forces in ply no. 2 as a function of the blank holder pressure.

Fig. 16 shows the evolution of wrinkles in the outer layer for two pressure levels. Despite the lower amount of defects in some layers, many wrinkles were predicted in both cases.

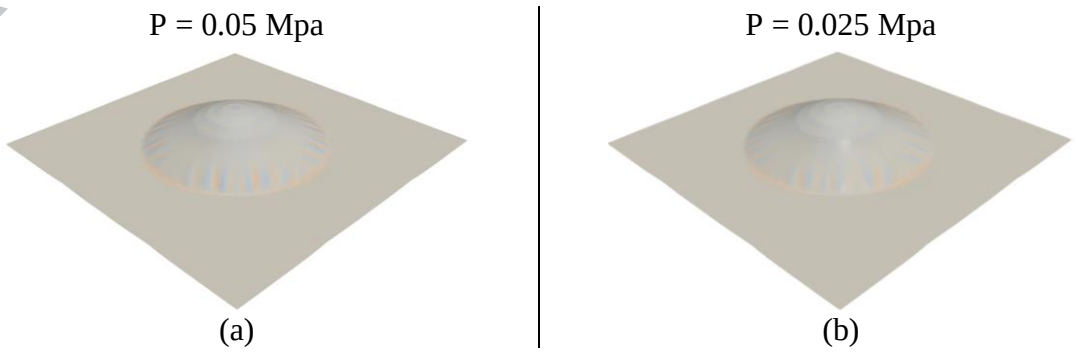

(a) (b)

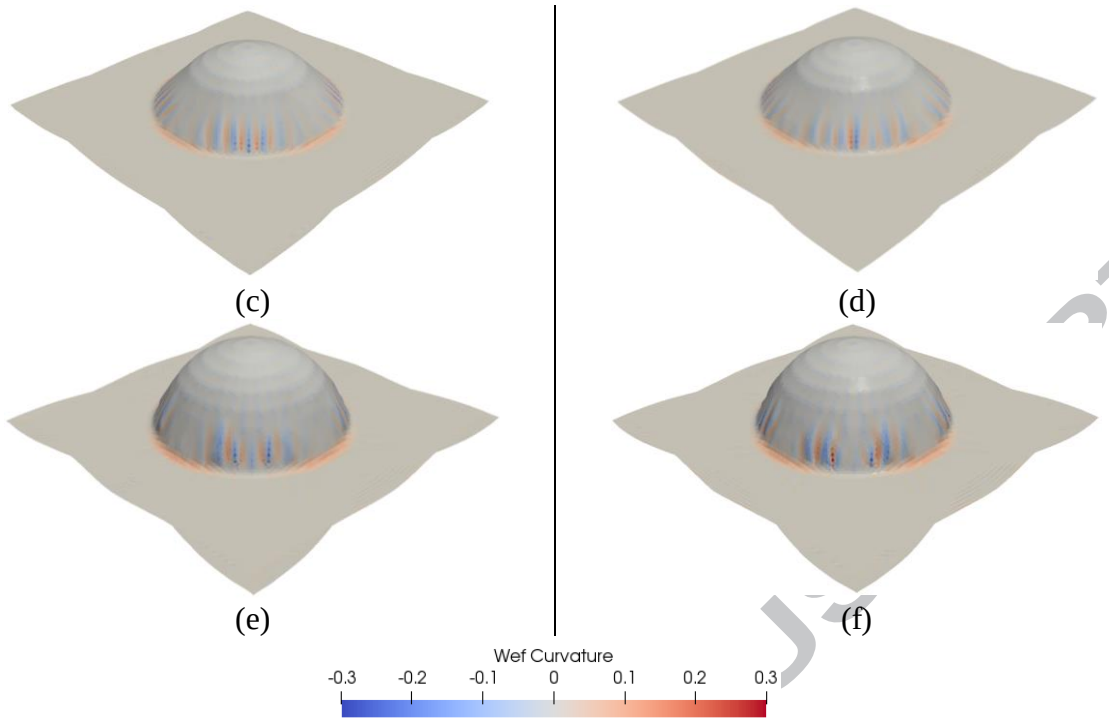

Fig. 16 Wrinkling development for 0.05 Mpa and 0.025 Mpa blank holder pressures

4.7 Some perspectives to reduce friction between layers

To reduce wrinkle phenomena, the above analyses show that it is important to reduce friction or to limit the interaction between layers. Recent experimental studies have analyzed the first option by introducing a mat fabric between the layers in order to diminish the effective friction coefficient [69]. Recently, a new process has been proposed to control layer separation during forming using active metal sheets between the fabric layers [70].

5. Conclusions

Friction associated with the varying types of deformation of two neighboring plies having different orientations are triggering mechanisms of wrinkling during forming of multi-layered composite reinforcements. Finite element simulations based on stress-resultant textile shell elements were able to accurately describe the onset and development of wrinkles during the forming processes. These simulations have shown that, during forming, zones of compression in the direction of the yarns resulting from friction forces were created by the slippage between neighboring plies having different orientations. The use of a blank holder to avoid wrinkles was

not straightforward. The increased tension due to the blank holder led to greater tension in the yarns but also to an increase in friction loads between the plies. Reducing friction between layers is one of the most serious ways to reduce wrinkling (Section 4.7).

It should also be emphasized that if the experiments give kinematic type results (wrinkle geometry), the numerical simulations of the forming give in addition results in terms of efforts and stresses. They are important because they are the ones that show in particular the compression forces in the tows during forming of multilayer reinforcement with different orientations.

In conclusion, wrinkling was increased during forming of a multi-layered composite reinforcement with different ply orientations. Numerical simulations could accurately predict the onset and development of wrinkles and determine, where possible, the conditions for a wrinkle-free manufacturing. Finally, it was important to reduce friction and normal loads between the plies.

References

[1] Hill, R., (1958). A general theory of uniqueness and stability in elastic-plastic solids. Journal of the Mechanics and Physics of Solids 6, 236–249. https://doi.org/10.1016/0022-5096(58)90029-2

[2] Wang, C.-T., Kinzel, G., Altan, T., (1994). Wrinkling criterion for an anisotropic shell with compound curvatures in sheet forming. International Journal of Mechanical Sciences 36, 945–960. https://doi.org/10.1016/0020-7403(94)90056-6

[3] Cao, J., Boyce, M.C., (1997). Wrinkling behavior of rectangular plates under lateral constraint. International Journal of Solids and Structures 34, 153–176. https://doi.org/10.1016/S0020-7683(96)00008-X

[4] Friedl, N., Rammerstorfer, F.G., Fischer, F.D., (2000). Buckling of stretched strips. Computers & Structures 78, 185–190. https://doi.org/10.1016/S0045-7949(00)00072-9

[5] Cerda, E., Mahadevan, L., (2003). Geometry and Physics of Wrinkling. Phys. Rev. Lett. 90, 074302. https://doi.org/10.1103/PhysRevLett.90.074302

[6] Amirbayat, J., Hearle, J.W.S., (1986). The complex buckling of flexible sheet materials—Part I. Theoretical approach. International Journal of Mechanical Sciences 28, 339–358. https://doi.org/10.1016/0020-7403(86)90054-8

[7] Amirbayat, J., & Hearle, J. W. S. (1989). The anatomy of buckling of textile fabrics: Drape and conformability. Journal of the Textile Institute, 80(1), 51-70. https://doi.org/10.1080/00405008908659185

[8] Clapp TG and Peng H. (1990) Buckling of woven fabrics .3. Experimental validation of theoretical models. Textile Research Journal;60(11):641-645.

https://doi.org/10.1177/004051759006001103
[9] Gutowski, T. G., Dillon, G., Chey, S., & Li, H. (1995). Laminate wrinkling scaling laws for ideal composites. Composites Manufacturing, 6(3-4), 123-134. https://doi.org/10.1016/0956-7143(95)95003-H
[10] Prodromou, A.G., Chen, J., (1997). On the relationship between shear angle and wrinkling of textile composite preforms. Composites Part A 28A, 491–503. https://doi.org/10.1016/S1359-835X(96)00150-9
[11] Rozant, O., Bourban, P.-E., Månson, J.-A.E., (2000). Drapability of dry textile fabrics for stampable thermoplastic preforms. Composites Part A: Applied Science and Manufacturing 31, 1167–1177. https://doi.org/10.1016/S1359-835X(00)00100-7
[12] Lebrun, G., Bureau, M.N., Denault, J., (2003). Evaluation of bias-extension and picture-frame test methods for the measurement of intraply shear properties of PP/glass commingled fabrics. Composite Structures 61, 341–352. https://doi.org/10.1016/S0263-8223(03)00057-6
[13] Sharma, S.B., Sutcliffe, M.P.F., Chang, S.H., (2003). Characterisation of material properties for draping of dry woven composite material. Composites Part A: Applied Science and Manufacturing 34, 1167–1175. https://doi.org/10.1016/j.compositesa.2003.09.001
[14] Hancock, S. G., & Potter, K. D. (2005). Inverse drape modelling—an investigation of the set of shapes that can be formed from continuous aligned woven fibre reinforcements. Composites Part A: Applied Science and Manufacturing, 36(7), 947-953. https://doi.org/10.1016/j.compositesa.2004.12.001
[15] Zhu, B., Yu, T.X., Teng, J., Tao, X.M., (2009). Theoretical modeling of large shear deformation and wrinkling of plain woven composite. Journal of composite materials 43, 125–138. https://doi.org/10.1177/0021998308098237
[16] Vanclooster, K., Lomov, S. V., & Verpoest, I. (2009). Experimental validation of forming simulations of fabric reinforced polymers using an unsymmetrical mould configuration. Composites Part A: Applied Science and Manufacturing, 40(4), 530-539. https://doi.org/10.1016/j.compositesa.2009.02.005
[17] Michaud V. (2012) Fibrous Preforms and Preforming, Wiley Encyclopedia of Composites Second Edition. Edited by L. Nicolais and A. Borzacchiello, John Wiley & Sons. https://doi.org/10.1002/9781118097298.weoc087
[18] Khan, M. A., Reynolds, N., Williams, G., & Kendall, K. N. (2015). Processing of thermoset prepregs for high-volume applications and their numerical analysis using superimposed finite elements. Composite Structures, 131, 917-926. https://doi.org/10.1016/j.compstruct.2015.06.056
[19] Hosseini, A., Kashani, M.H., Sassani, F., Milani, A.S., Ko, F., (2017). A Mesoscopic Analytical Model to Predict the Onset of Wrinkling in Plain Woven Preforms under Bias Extension Shear Deformation. Materials (Basel) 10. https://doi.org/10.3390/ma10101184
[20] Gatouillat, S., Bareggi, A., Vidal-Sallé, E., & Boisse, P. (2013). Meso modelling for composite preform shaping–simulation of the loss of cohesion of the woven fibre network. Composites Part A: Applied science and manufacturing, 54, 135-144. https://doi.org/10.1016/j.compositesa.2013.07.010
[21] Alsayednoor, J., Lennard, F., Yu, W.R., Harrison, P., (2017). Influence of specimen pre-shear and wrinkling on the accuracy of uniaxial bias extension test results. Composites Part A: Applied Science and Manufacturing 101, 81–97. https://doi.org/10.1016/j.compositesa.2017.06.006
[22] Hosseini, A., Kashani, M.H., Sassani, F., Milani, A.S., Ko, F.K., (2018). Identifying the

distinct shear wrinkling behavior of woven composite preforms under bias extension and picture frame tests. Composite Structures 185, 764–773. https://doi.org/10.1016/j.compstruct.2017.11.033

[23] Boisse, P., Hamila, N., Vidal-Sallé, E., Dumont, F., (2011). Simulation of wrinkling during textile composite reinforcement forming. Influence of tensile, in-plane shear and bending stiffnesses. Composites Science and Technology 71, 683–692. https://doi.org/10.1016/j.compscitech.2011.01.011

[24] Boisse, P., Hamila, N., Guzman-Maldonado, E., Madeo, A., Hivet, G., & Dell'Isola, F. (2017). The bias-extension test for the analysis of in-plane shear properties of textile composite reinforcements and prepregs: a review. International Journal of Material Forming, 10(4), 473-492. https://doi.org/10.1007/s12289-016-1294-7

[25] Cherouat, A., Billoët, J.L., (2001). Mechanical and numerical modelling of composite manufacturing processes deep-drawing and laying-up of thin pre-impregnated woven fabrics. Journal of Materials Processing Technology 118, 460–471. https://doi.org/10.1016/S0924-0136(01)00987-6

[26] Skordos, A.A., Aceves, C.M., Sutcliffe, M.P.F., (2007). A simplified rate dependent model of forming and wrinkling of pre-impregnated woven composites. Composites Part A: Applied Science and Manufacturing 38, 1318–1330. https://doi.org/10.1016/j.compositesa.2006.11.005

[27] Jauffrès, D., Sherwood, J. A., Morris, C. D., & Chen, J. (2010). Discrete mesoscopic modeling for the simulation of woven-fabric reinforcement forming. International Journal of Material Forming, 3(2), 1205-1216. https://doi.org/10.1007/s12289-009-0646-y

[28] Dangora, L. M., Mitchell, C. J., & Sherwood, J. A. (2015). Predictive model for the detection of out-of-plane defects formed during textile-composite manufacture. Composites Part A: Applied Science and Manufacturing, 78, 102-112. https://doi.org/10.1016/j.compositesa.2015.07.011

[29] Harrison, P. (2016). Modelling the forming mechanics of engineering fabrics using a mutually constrained pantographic beam and membrane mesh. Composites Part A: Applied Science and Manufacturing, 81, 145-157. https://doi.org/10.1016/j.compositesa.2015.11.005

[30] Beakou, A., Cano, M., Le Cam, J. B., & Verney, V. (2011). Modelling slit tape buckling during automated prepreg manufacturing: A local approach. Composite structures, 93(10), 2628-2635. https://doi.org/10.1016/j.compstruct.2011.04.030

[31] Lightfoot, J.S., Wisnom, M.R., Potter, K., (2013). A new mechanism for the formation of ply wrinkles due to shear between plies. Composites Part A: Applied Science and Manufacturing 49, 139–147. https://doi.org/10.1016/j.compositesa.2013.03.002

[32] Lightfoot, J. S., Wisnom, M. R., & Potter, K. (2013). Defects in woven preforms: Formation mechanisms and the effects of laminate design and layup protocol. Composites Part A: Applied Science and Manufacturing, 51, 99-107. https://doi.org/10.1016/j.compositesa.2013.04.004

[33] Hallander, P., Akermo, M., Mattei, C., Petersson, M., Nyman, T., (2013). An experimental study of mechanisms behind wrinkle development during forming of composite laminates. Composites Part A: Applied Science and Manufacturing 50, 54–64. https://doi.org/10.1016/j.compositesa.2013.03.013

[34] Dodwell, T.J., Butler, R., Hunt, G.W., (2014). Out-of-plane ply wrinkling defects during consolidation over an external radius. Composites Science and Technology 105, 151–159. https://doi.org/10.1016/j.compscitech.2014.10.007

[35] Haanappel, S. P., Ten Thije, R. H. W., Sachs, U., Rietman, B., & Akkerman, R. (2014). Formability analyses of uni-directional and textile reinforced thermoplastics. Composites Part A: Applied Science and Manufacturing, 56, 80-92. https://doi.org/10.1016/j.compositesa.2013.09.009

[36] Hallander, P., Sjölander, J., Åkermo, M., (2015). Forming induced wrinkling of composite laminates with mixed ply material properties; an experimental study. Composites Part A: Applied Science and Manufacturing 78, 234–245. https://doi.org/10.1016/j.compositesa.2015.08.025

[37] Chen, S., McGregor, O. P. L., Harper, L. T., Endruweit, A., & Warrior, N. A. (2016). Defect formation during preforming of a bi-axial non-crimp fabric with a pillar stitch pattern. Composites Part A: Applied Science and Manufacturing, 91, 156-167. https://doi.org/10.1016/j.compositesa.2016.09.016

[38] Leutz, D., Vermilyea, M., Bel, S., Hinterhölzl, R., (2016). Forming Simulation of Thick AFP Laminates and Comparison with Live CT Imaging. Appl Compos Mater 23, 583–600. https://doi.org/10.1007/s10443-016-9475-6

[39] Sjölander, J., Hallander, P., Åkermo, M., (2016). Forming induced wrinkling of composite laminates: A numerical study on wrinkling mechanisms. Composites Part A: Applied Science and Manufacturing 81, 41–51. https://doi.org/10.1016/j.compositesa.2015.10.012

[40] Farnand, K., Zobeiry, N., Poursartip, A., & Fernlund, G. (2017). Micro-level mechanisms of fiber waviness and wrinkling during hot drape forming of unidirectional prepreg composites. Composites Part A: Applied Science and Manufacturing, 103, 168-177. https://doi.org/10.1016/j.compositesa.2017.10.008

[41] Belnoue, J.P.-H., Mesogitis, T., Nixon-Pearson, O.J., Kratz, J., Ivanov, D.S., Partridge, I.K., Potter, K.D., Hallett, S.R., (2017). Understanding and predicting defect formation in automated fibre placement pre-preg laminates. Composites Part A: Applied Science and Manufacturing 102, 196–206. https://doi.org/10.1016/j.compositesa.2017.08.008

[42] Belnoue, J. H., Nixon-Pearson, O. J., Thompson, A. J., Ivanov, D. S., Potter, K. D., & Hallett, S. R. (2018). Consolidation-driven defect generation in thick composite parts. Journal of Manufacturing Science and Engineering, 140(7), 071006. doi: 10.1115/1.4039555

[43] Sadighi, M., Rabizadeh, E., Kermansaravi, F., (2008). Effects of laminate sequencing on thermoforming of thermoplastic matrix composites. Journal of Materials Processing Technology, 201, 725–730. https://doi.org/10.1016/j.jmatprotec.2007.11.239

[44] ten Thije, R.H.W., Akkerman, R., (2009). A multi-layer triangular membrane finite element for the forming simulation of laminated composites. Composites Part A: Applied Science and Manufacturing 40, 739–753. https://doi.org/10.1016/j.compositesa.2009.03.004

[45] Vanclooster, K., Lomov, S.V., Verpoest, I., (2009). On the formability of multi-layered fabric composites, in: ICCM—17th International Conference on Composite Materials, Edinburgh, UK.

[46] Vanclooster, K., Lomov, S. V., & Verpoest, I. (2010). Simulation of multi-layered composites forming. International Journal of Material Forming, 3(1), 695-698. https://doi.org/10.1007/s12289-010-0865-2

[47] De Luca P, Lefébure P and Pickett AK. (1998) Numerical and experimental investigation of some press forming parameters of two fibre reinforced thermoplastics: Apc2-as4 and pei-cetex. Composites Part A: Applied Science and Manufacturing, 29(1-2):101-110. https://doi.org/10.1016/S1359-835X(97)00060-2

[48] Allaoui, S., Cellard, C., Hivet, G., (2015). Effect of inter-ply sliding on the quality of multilayer interlock dry fabric preforms. Composites Part A: Applied Science and Manufacturing 68, 336–345. https://doi.org/10.1016/j.compositesa.2014.10.017

[49] Nezami, F.N., Gereke, T., Cherif, C., (2016). Analyses of interaction mechanisms during forming of multilayer carbon woven fabrics for composite applications. Composites Part A: Applied Science and Manufacturing 84, 406–416. https://doi.org/10.1016/j.compositesa.2016.02.023

[50] Hughes, T.J.R., Belytschko, T., (1983). A precis of developments in computational methods for transient analysis. Journal of Applied Mechanics 50, 1033–1041. doi:10.1115/1.3167186

[51] Crisfield, M. A., Remmers, J. J., & Verhoosel, C. V. (2012). Nonlinear finite element analysis of solids and structures. John Wiley & Sons.

[52] Hamila, N., Boisse, P., Sabourin, F., Brunet, M., (2009). A semi-discrete shell finite element for textile composite reinforcement forming simulation. International Journal for Numerical Methods in Engineering 79, 1443–1466. https://doi.org/10.1002/nme.2625

[53] Boisse, P., Hamila, N., Helenon, F., Hagège, B., & Cao, J. (2008). Different approaches for woven composite reinforcement forming simulation. International Journal of Material Forming, 1(1), 21-29. https://doi.org/10.1007/s12289-008-0002-7

[54] Syerko, E., Comas-Cardona, S., & Binetruy, C. (2012). Models of mechanical properties/behavior of dry fibrous materials at various scales in bending and tension: A review. Composites Part A: Applied Science and Manufacturing, 43(8), 1365-1388. https://doi.org/10.1016/j.compositesa.2012.03.012

[55] Liang, B., Hamila, N., Peillon, M., & Boisse, P. (2014). Analysis of thermoplastic prepreg bending stiffness during manufacturing and of its influence on wrinkling simulations. Composites Part A: Applied Science and Manufacturing, 67, 111-122. https://doi.org/10.1016/j.compositesa.2014.08.020

[56] Ouagne, P., Soulat, D., Tephany, C., & Gillibert, J. (2016). Measurement of the appearance and growth of tow buckling defect in the frame of complex shape manufacturing process by using fringe projection technique. Strain, 52(6), 559-569. https://doi.org/10.1111/str.12206

[57] Alshahrani, H., & Hojjati, M. (2017). A theoretical model with experimental verification for bending stiffness of thermosetting prepreg during forming process. Composite Structures, 166, 136-145. https://doi.org/10.1016/j.compstruct.2017.01.030

[58] Boisse, P., Colmars, J., Hamila, N., Naouar, N., & Steer, Q. (2018). Bending and wrinkling of composite fiber preforms and prepregs. A review and new developments in the draping simulations. Composites Part B: Engineering, 141, 234–249, https://doi.org/10.1016/j.compositesb.2017.12.061

[59] Kärger, L., Galkin, S., Zimmerling, C., Dörr, D., Linden, J., Oeckerath, A., & Wolf, K. (2018). Forming optimisation embedded in a CAE chain to assess and enhance the structural performance of composite components. Composite Structures, 192, 143-152. https://doi.org/10.1016/j.compstruct.2018.02.041

[60] Onate, E., Zarate, F., (2000). Rotation-free triangular plate and shell elements. International Journal for Numerical Methods in Engineering 47, 557–603.

[61] Marjanović, M., & Vuksanović, D. (2016). Free vibrations of laminated composite shells using the rotation-free plate elements based on Reddy's layerwise discontinuous displacement model. Composite Structures, 156, 320-332. https://doi.org/10.1016/j.compstruct.2015.07.125

[62] Bel, S., Hamila, N., Boisse, P., & Dumont, F. (2012). Finite element model for NCF composite reinforcement preforming: Importance of inter-ply sliding. *Composites Part A: Applied science and manufacturing*, *43*(12), 2269-2277. http://dx.doi.org/10.1016/j.compositesa.2012.08.005

[63] Gorczyca-Cole, J. L., Sherwood, J. A., & Chen, J. (2007). A friction model for thermostamping commingled glass–polypropylene woven fabrics. Composites Part A: applied science and manufacturing, 38(2), 393-406. https://doi.org/10.1016/j.compositesa.2006.03.006

[64] Wang, P., Hamila, N., & Boisse, P. (2013). Thermoforming simulation of multilayer composites with continuous fibres and thermoplastic matrix. Composites Part B: Engineering, 52, 127-136. https://doi.org/10.1016/j.compositesb.2013.03.045

[65] Breuer, U., Neitzel, M., Ketzer, V., Reinicke, R., (1996). Deep drawing of fabric-reinforced thermoplastics: Wrinkle formation and their reduction. Polym Compos 17, 643–647. https://doi.org/10.1002/pc.10655

[66] Obermeyer, E. J., & Majlessi, S. (1998). A review of recent advances in the application of blank-holder force towards improving the forming limits of sheet metal parts. Journal of Materials Processing Technology, 75(1-3), 222-234. https://doi.org/10.1016/S0924-0136(97)00368-3

[67] Lee, J.S., Hong, S.J., Yu, W.-R., Kang, T.J., (2007). The effect of blank holder force on the stamp forming behavior of non-crimp fabric with a chain stitch. Composites Science and Technology 67, 357–366. https://doi.org/10.1016/j.compscitech.2006.09.009

[68] Lin, H., Wang, J., Long, C., Clifford, M.J., Harrison, P., (2007). Predictive modelling for optimization of textile composite forming. Composites Science and Technology 67, 3242–3252. https://doi.org/10.1016/j.compscitech.2007.03.040

[69] Shanwan, A., Allaoui, S., (2018). Different experimental ways to minimize the preforming defects of multi-layered interlock dry fabric. Int J Mater Form 1–10. https://doi.org/10.1007/s12289-018-1407-6

[70] Nezami, F.N., Gereke, T., Cherif, C., (2017). Active forming manipulation of composite reinforcements for the suppression of forming defects. Composites Part A: Applied Science and Manufacturing 99, 94–101. https://doi.org/10.1016/j.compositesa.2017.04.011